/lmg

PS/BT/Note 87-5
26.10.1987

AA INJECTION KICKER SYSTEM FOR AA COMPLEX

K.D. Metzmacher
L. Sermeus

ABSTRACT

As a consequence of the construction of an Antiproton Collector, it has been possible to simplify the AA injection kicker system. This note describes the new system built and gives the useful parameters to run it.

1. INTRODUCTION

This note describes the kicker system built for the injection of antiprotons from the AC ring into the AA ring for the ACOL project.

The previously ten AA injection kicker magnet modules located in tanks K3 and K4 [1] have been replaced by four magnet modules located in tank K4 only (Fig. 1). Advantage was taken of the reduced beam dimensions and the longer permissible kick fall time (180 ns instead of 80 ns).

2. BEAM REQUIREMENTS

After cooling in the AC ring, the antiproton beam is rebunched in a single bunch of 360 ns length.

- AA rotation time being 540 ns, this leaves 180 ns fall time (95-5%) permissible for the kick, assuming that 95% of the full kick will touch the last particles of the bunch to be injected and 5% the first particles which complete their first turn in the ring.

- The deflection angle requested is θ = 7,034 mrad for a 25 π mm.mrad,

  $\frac{\Delta P}{P}$ = 0,025% injected beam. ($\int Bdl$ = 0,08385 T.m).

- A field uniformity of $\pm$ 1% is also requested inside the useful aperture.

- Furthermore, the old K4 tank including all his shutter movement parts is reused. This imposes dimensional constraints on the mechanical design of the kicker modules.

3. MAGNETS

3.1 Design

According to the beam dimensions [2], the kick strength required and the kick fall time allowed, it appeared that the design of four identical kicker modules was the most convenient and economical.

The magnet construction follows closely that used before. Briefly, this means transmission line type magnets made of C-core Philips 8C11 ferrites, interleaved high tension (HT) and earth (E) "mirror finish" aluminium magnesium alloy plates (ALMg3), alumina (Al_2O_3) insulation and an outer stainless steel support frame (Fig. 2).

The whole assembly is bakeable to 300^0C in situ. Each module is of open C-aperture design and has 17 mechanically identical cells. The characteristic impedance is 15Ω and is imposed by the already existing generator.

In order to define a "good" field region with a uniformity of $\pm$1%, the C-core and conductor shapes have been designed with the help of computer programs MAGNET and POISSON. These calculations were checked by RF low voltage measurements on a model magnet. A plot of flux

lines given by POISSON is shown in Fig. 3. A plot of computed field uniformity and the beam envelope at magnet entry and exit is given for each module in Fig. 4. The screening effect of the earth conductor allows to reduce the leakage field to 0,23% (calculated) of the nominal field on the equilibrium orbit, shutter open. The use of this shutter should not be necessary because the stray field is lower now than it was with the shutter closed previously. A plot of field decrease is given in Fig. 5.

Table 1 gives a summary of the main magnet characteristics.

3.2 Pulse Generators

Each magnet is powered from a 15Ω cable PFN pulse generator and terminated by a 15Ω load (Fig. 6). Generator and load are each connected to the magnet via two 30Ω cables in parallel.

For certain operations kick polarity reversal is necessary. This is achieved by current direction reversal in the magnets. This requires exchanging the generator for the load transmission cables and vice versa.

Normal operation at nominal deflection angle of 2,63 mrad per module is with four pulse generators at 53 kV. Any three out of four generators at 70 kV will also suffice. Maximum possible operating voltage is 80 kV, thus providing acceptable margin.

3.3 Performance

All low voltage and high voltage measurements performed give results in good accordance with the calculations.

a) L.V. measurements

These measurements have been performed with a HP pulse generator feeding the magnet terminated with 15Ω. The 50Ω generator, was matched to the magnet via a resistive divider. A pulse having the following characteristics has been applied (Fig. 7).

Rise time (10 - 90%)	: 35 ns
Fall time (90 - 10%)	: 40 ns
Width (50%)	: 500 ns
Amplitude	: 1,6 V

The propagation of the falling edge of this pulse through the magnet cells is shown in Fig. 8. The traces represent the voltage measured on particular HT plates which are separated by the ferrite blocks. The very first and last lines are measured at the magnet connections.

The integrated field ($\int Bdl$) can be measured by two methods :

- Numerical integrated voltage across the magnet (Fig. 9).

- Measurement of the field inside the aperture with a strip line short circuited at one end and terminated at the other end. Four

short circuited at one end and terminated at the other end. Four measurements can be taken with this method according to the sense of the travelling wave in the probe with respect to the magnet and according to which strip conductor is earthed. A sum of these four measurements gives the best result because it eliminates nearly all the parasitic effects (Fig. 10). The probe gives $\frac{d\phi}{dt}$ which is numerically integrated to obtain $\int Bdl$.

The field uniformity has been measured with the same probe. The magnet was excited by a sine wave of 1,5 MHz frequency. The results are shown in Fig. 11. The field uniformity of $\pm$ 1% is as requested except in the corners near the HT conductor, positions where particles do not circulate (elliptic beam cross-section).

b) H.V. measurements

After bake-out to 300^0C, magnets have been tested at HV in order to measure their performance in conditions close to future operation.

The test voltage was 80 kV which is the maximum voltage which can be used in operation, the corresponding current being roughly 2600 A.

A typical $\int Bdl$ photo measured with a strip line probe is shown in Fig. 12. An estimation of the kick based on this photo gives 326 G.m, the calculated value being 324 G.m. A fall time of $\approx$ 100 ns (90 - 10)% can be observed and a 700 ns plateau maximum length at 100% $\pm$ 0,5% kick is available. Unfortunately, unavoidable mismatches between generator, transmissions, connection boxes, magnet and terminator exist and disturb the kick rise and fall. This can be well calculated with the SPICE program. The equivalent circuit used in this simulation is shown in Fig. 13 and the kick is plotted in Fig. 14. The actual matching has been improved by connecting a capacitor in parallel with the terminator (Fig. 15).

c) Magnet installation in K4

The magnets have been positioned in the tank (Fig. 16) in such a way that the existing feet positions and feedthroughs could be reused. To fit the good field region of the apertures with respect to the beam location, there is a radial shift of a few mm from one magnet to the next (Fig. 17). Furthermore, on special AA request (H. Koziol), a shift of 8 mm radially outside has been given to the magnets because beam observed in the previous AA version was so shifted (this shift is not represented in Fig. 17). The leakage field on the equilibrium orbit measured was .04% of the main field. This value is much smaller than the computed one given in paragraph 3.1.

REFERENCES

1. The injection kicker system of the CERN Antiproton Accumulator, D.C. Fiander et al, CERN/PS/EI 81-8.

2. AA Beam dimensions including injected and ejected beams, M. Martini, PS/ACOL/Note 42.

3. R. Sherwood, Private communications.

Drawings : PS-A22-1153-O Ensemble K4/I-II-III-IV.

PS-A22-1159-2A Disposition des aimants dans le tank.

Distribution :

AA Group Scientific Staff
BT Group Scientific Staff

TABLE 1 : AA INJECTION

DATA	UNITS	K4-I, II, III, IV
w (w_{eff})	mm	110 (132)
h	mm	45
n	cells	17
l (l_{eff})	mm	408 (432)
Z_o	Ω	15
PFN	kV	80
I	A	2600
θ	mrad	2.63
∫Bdl	T.m	.03136
L	μH	1.59
C	pF	7077
T_M	ns	106,2
B_{air}	T	.0726
w_{fer}	mm	60
$B_{fer\ mid\ cell}$	T	.2061
$B_{fer\ end\ cell}$	T	.3091
V_{fer}	cm^3	8440
M_{fer}	kg	45
$B_{rem}.l$	T.m	75×10^{-6}
A_{mag}	mm x mm	525 x 778
l_{mag}	mm	452

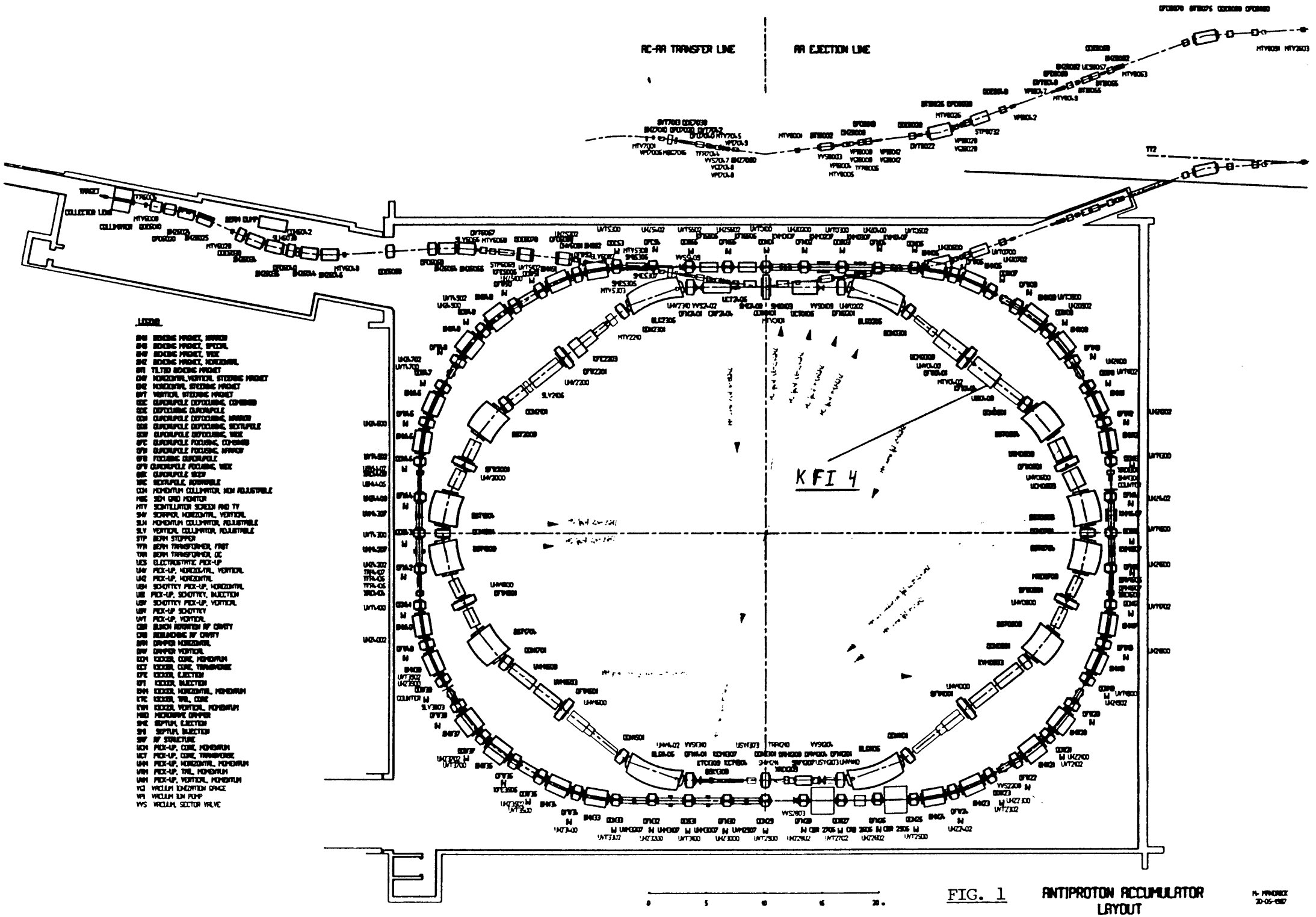

FIG. 1 ANTIPROTON ACCUMULATOR LAYOUT

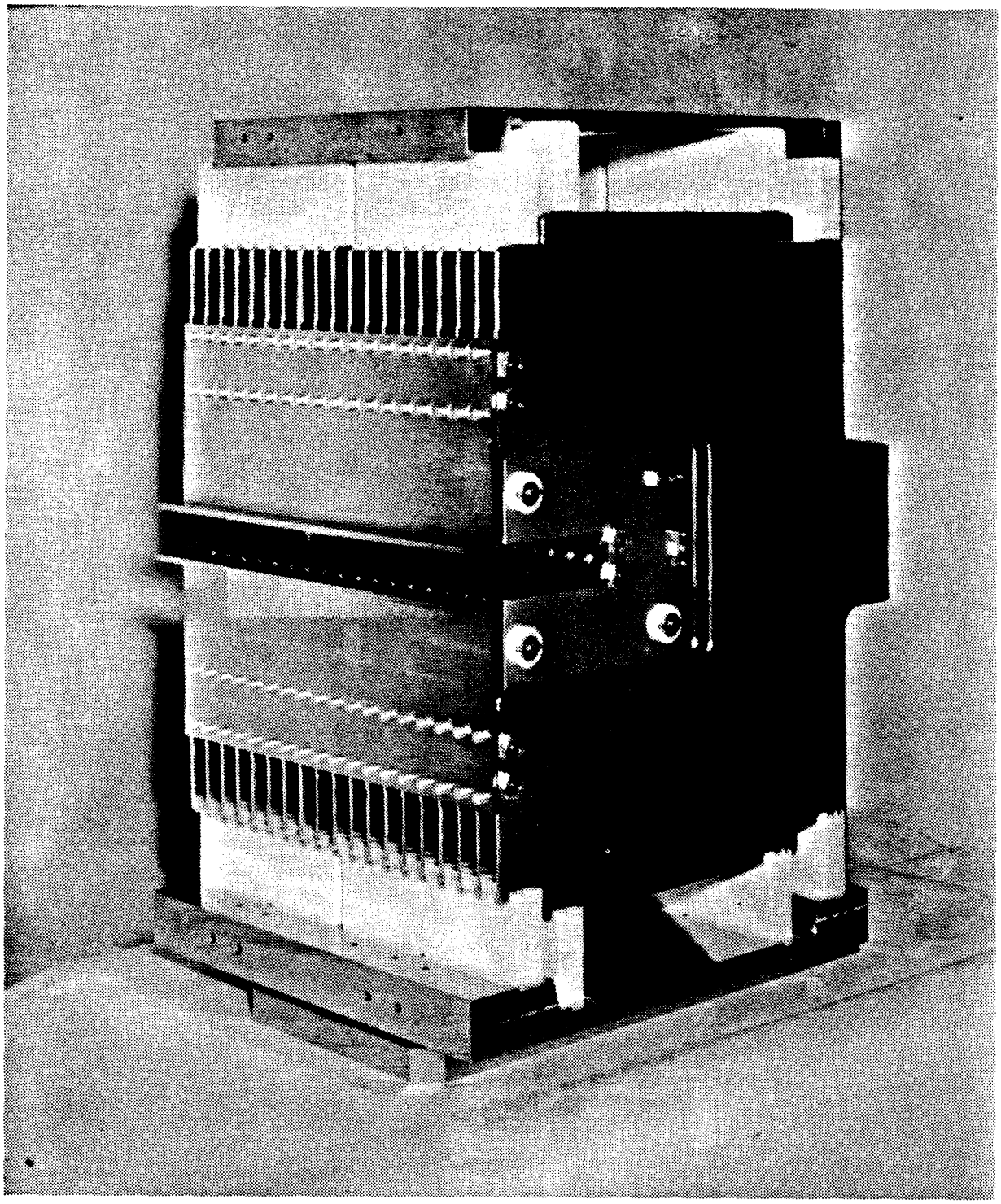

FIG. 2 Magnet module.

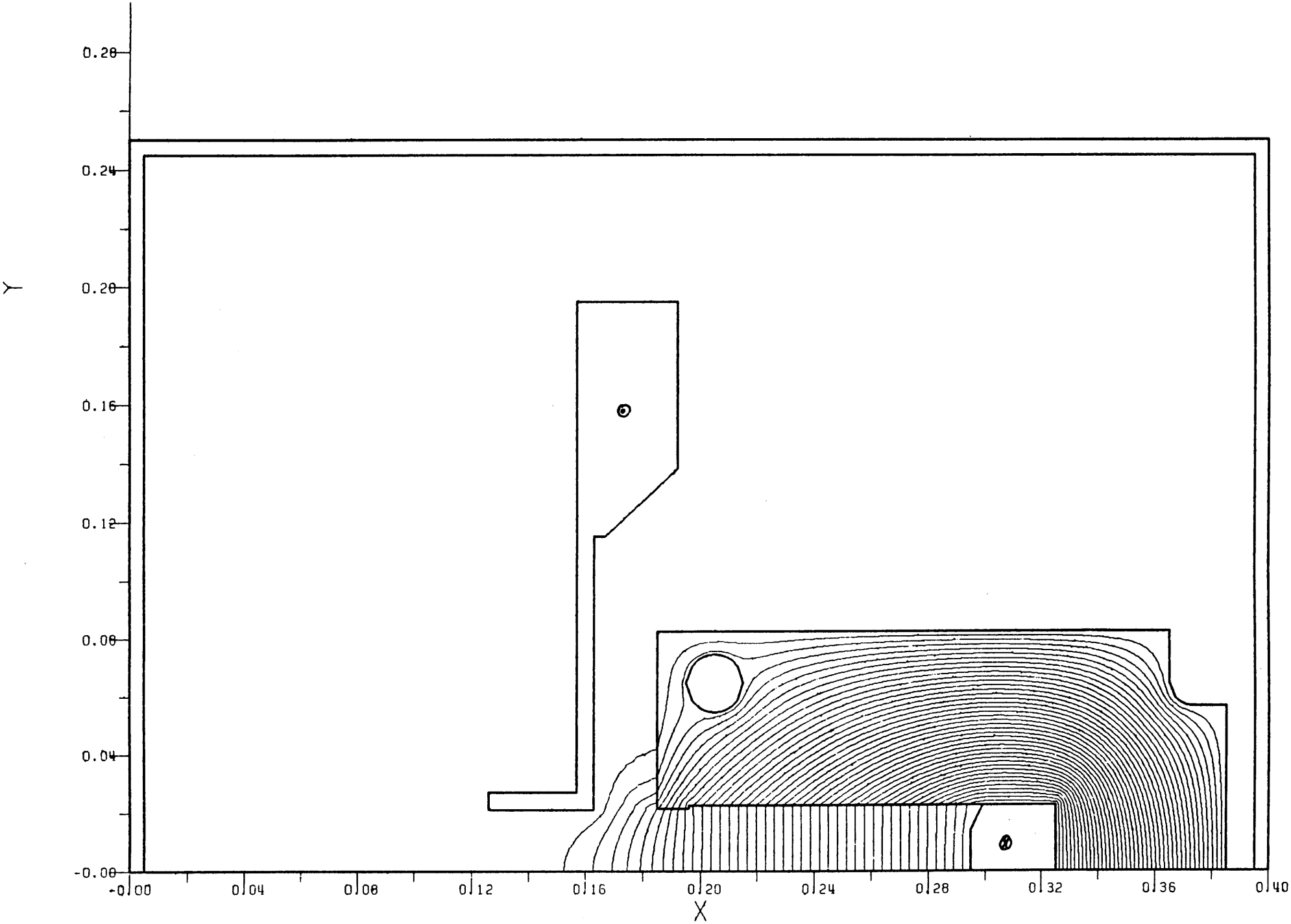

FIG. 3 POISSON plot of flux lines.

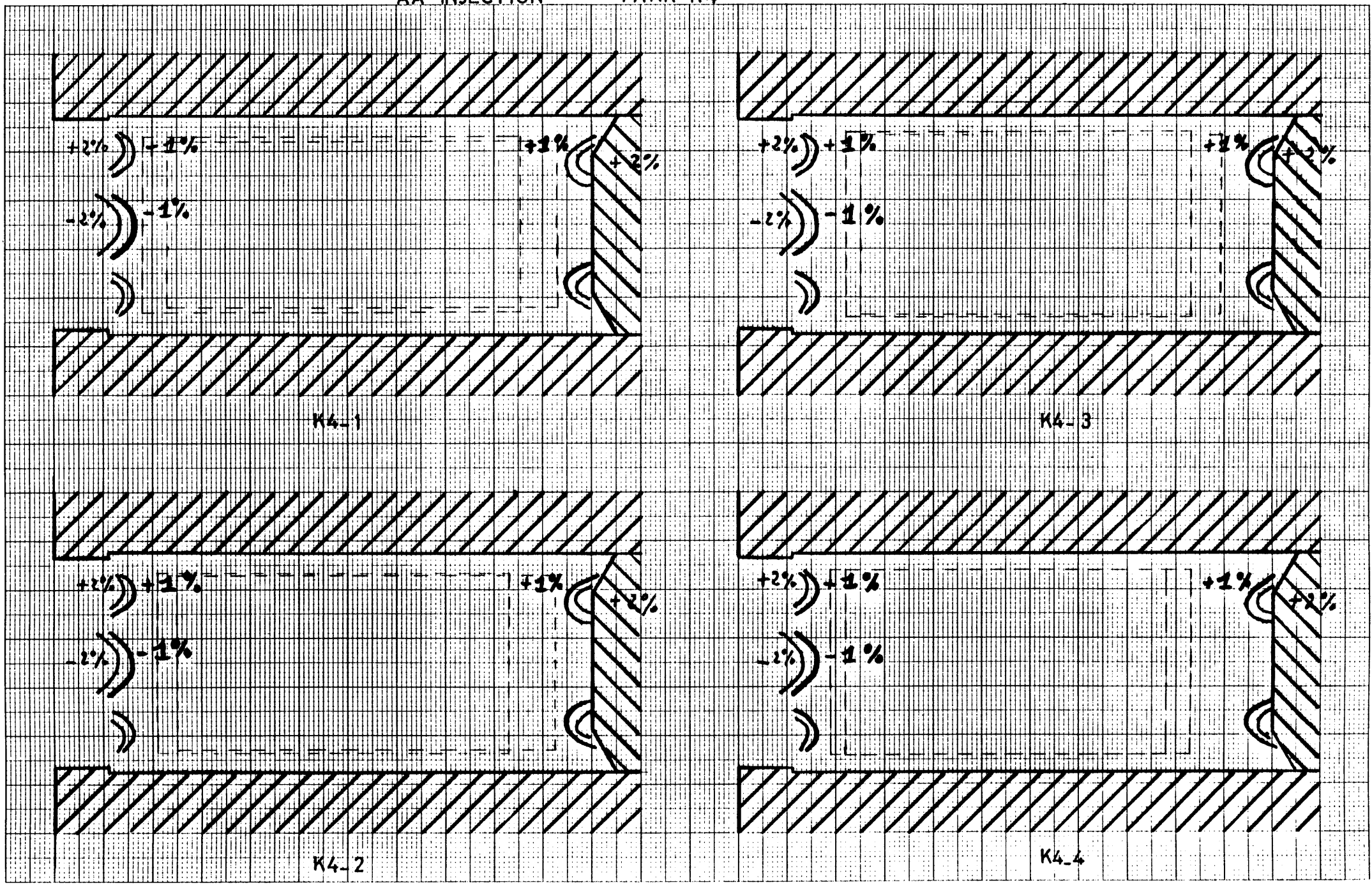

FIG. 4 Field uniformity and beam envelope.

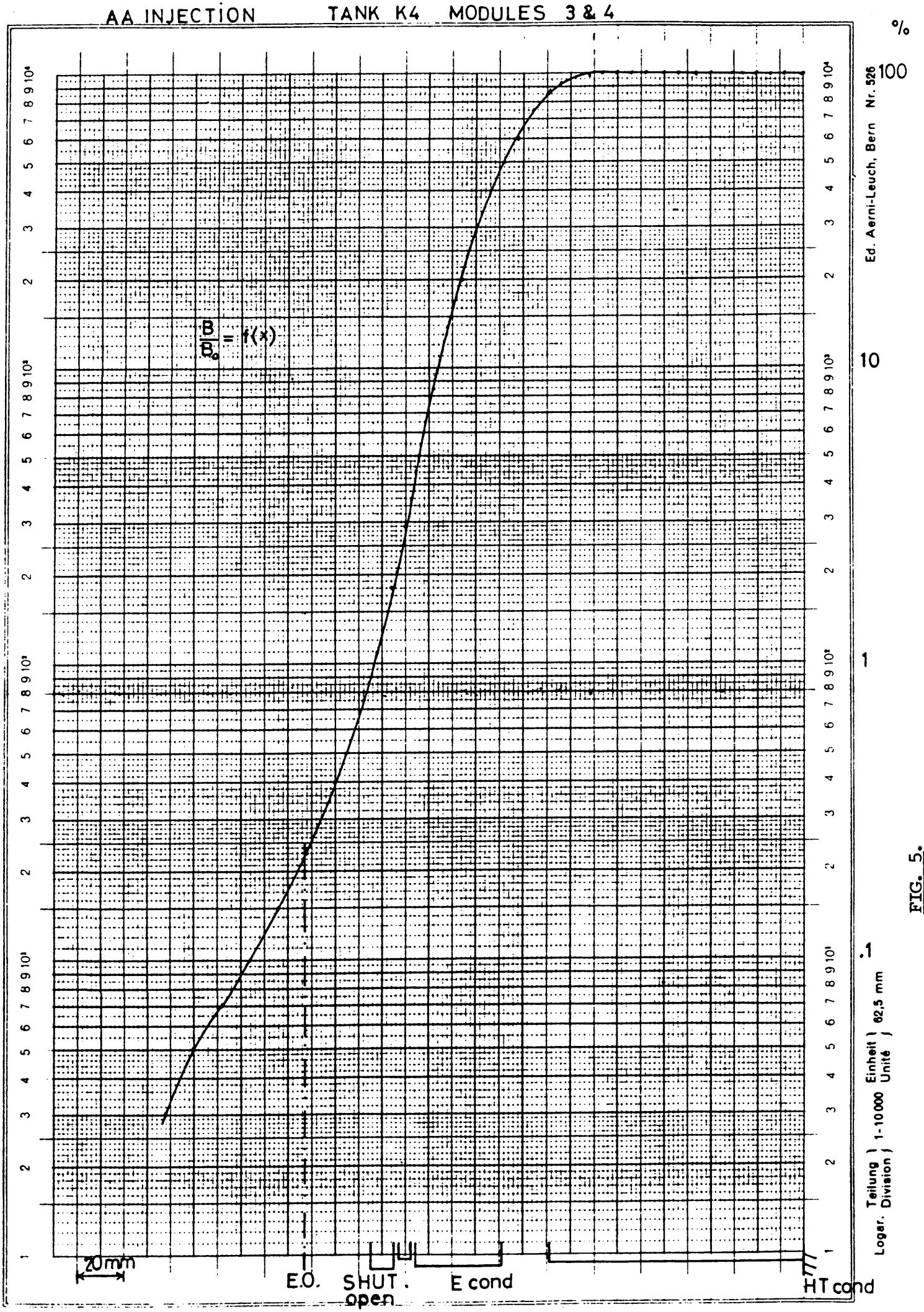
AA INJECTION TANK K4 MODULES 3 & 4
%
100
10
1
.1
$\frac{B}{B_o} = f(x)$
20 mm
E.O.
SHUT. open
E cond
HT cond
Ed. Aerni-Leuch, Bern Nr. 526
Logar. Teilung / 1-10000 Einheit / 62,5 mm
Division / Unité /

FIG. 5.

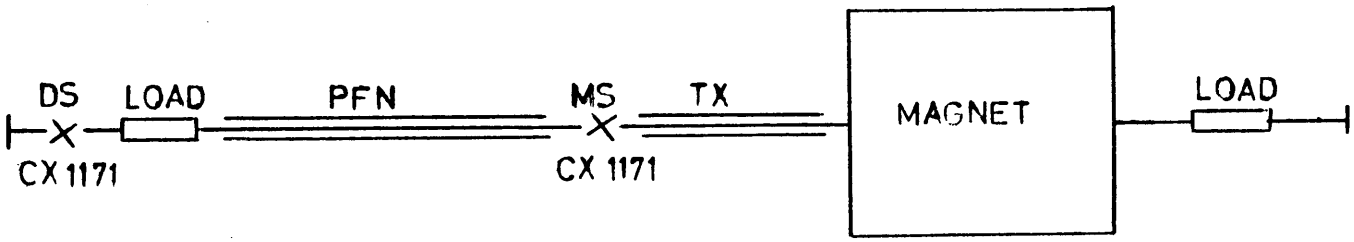

FIG. 6 Pulse generator

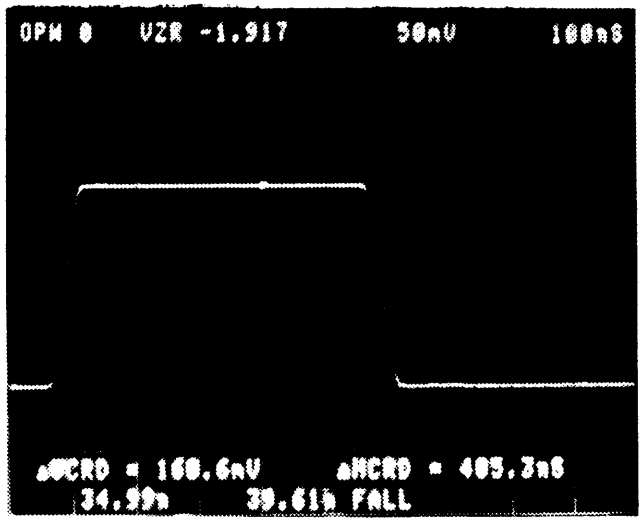

FIG. 7 L.V. Input pulse.

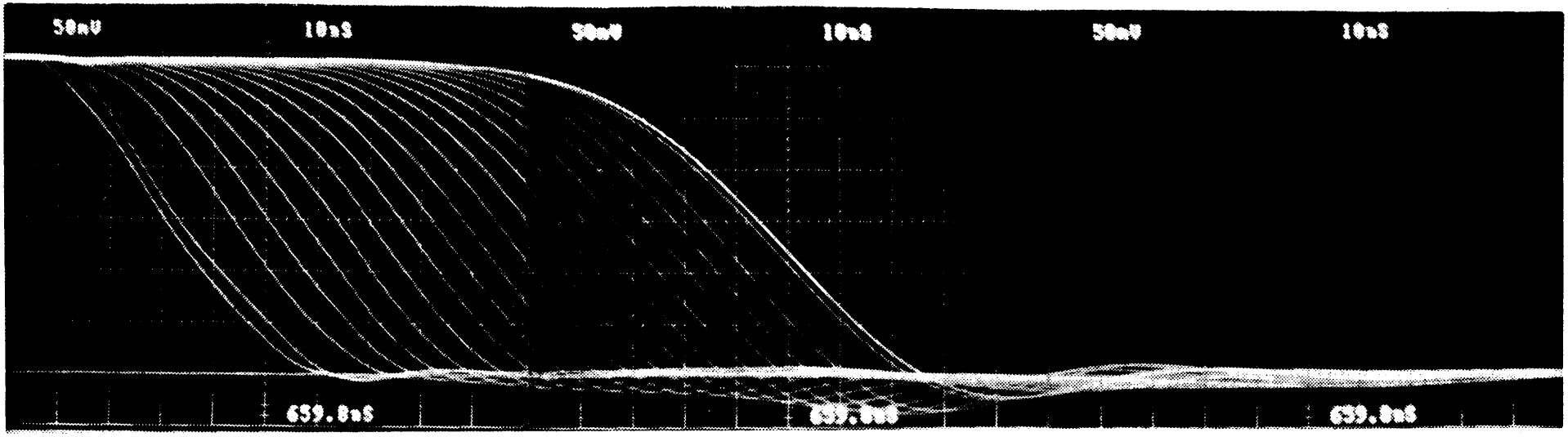

FIG. 8 Pulse propagation.

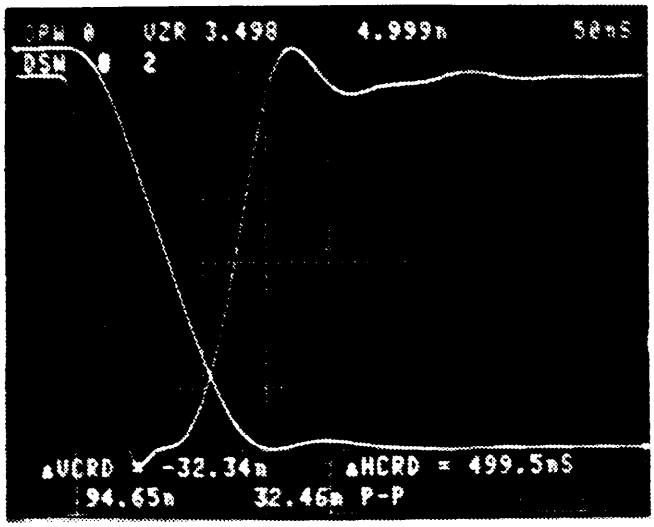

FIG. 9 L.V. $e_1 - e_{18}$ and $\int(e_1 - e_{18})dt$.

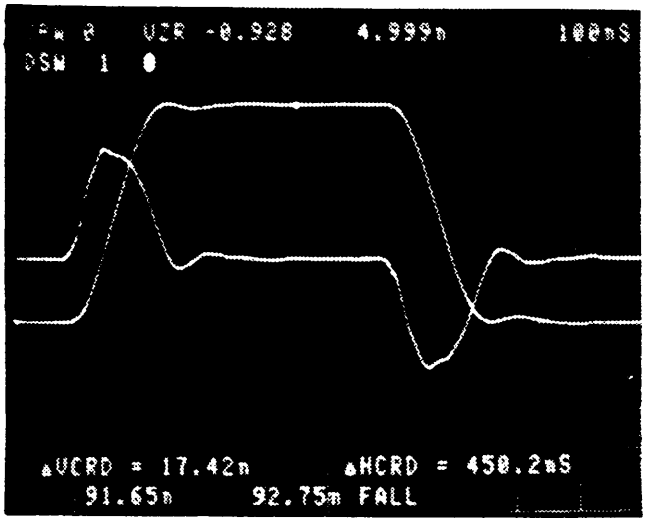

FIG. 10 L.V. $\int Bdl$

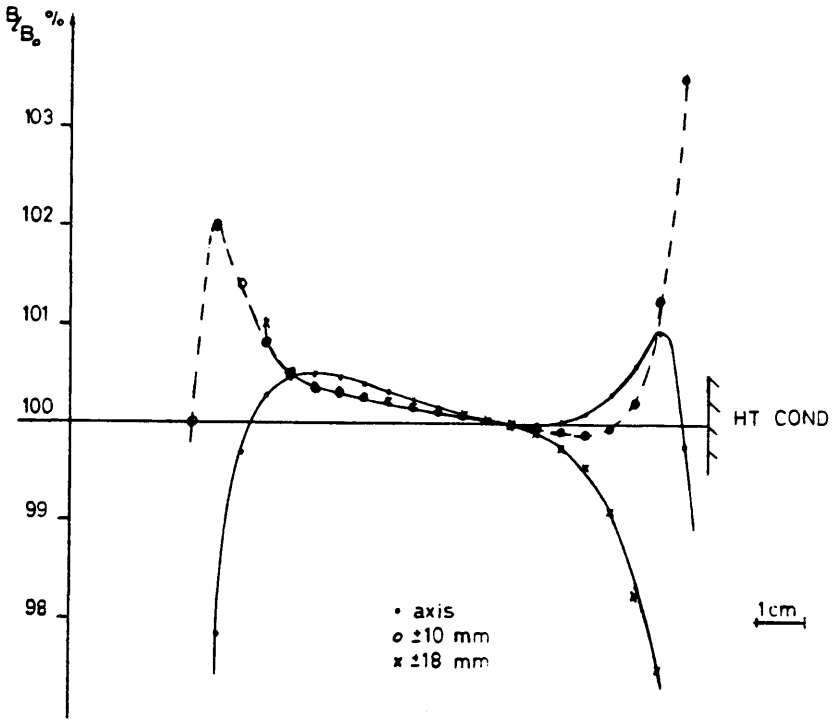

FIG. 11 Field uniformity.

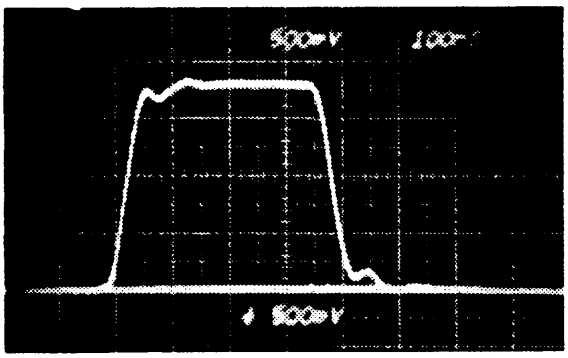

FIG. 12 H.V. $\int Bdl$.

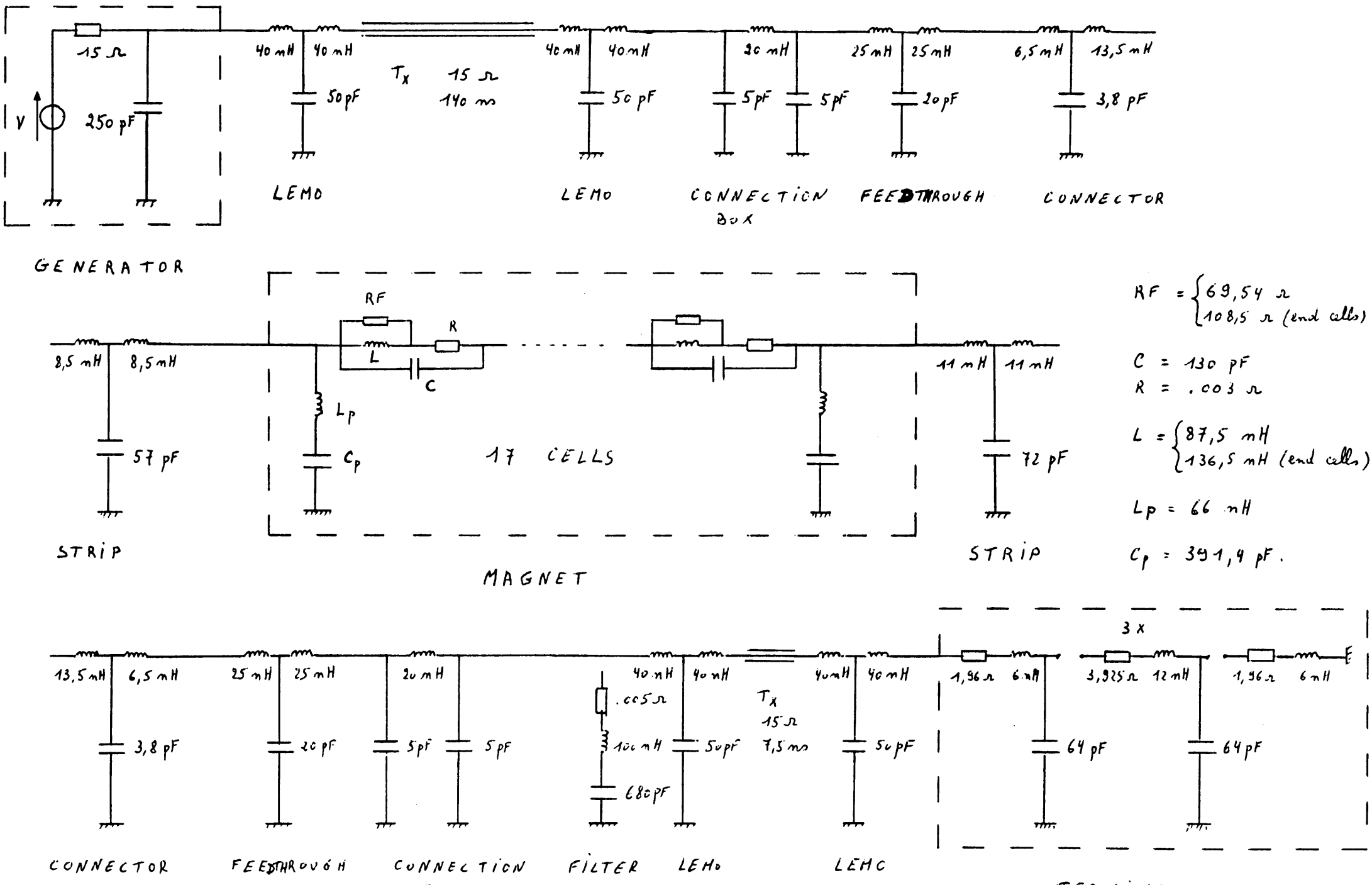

FIG. 13 SPICE equivalent circuit.

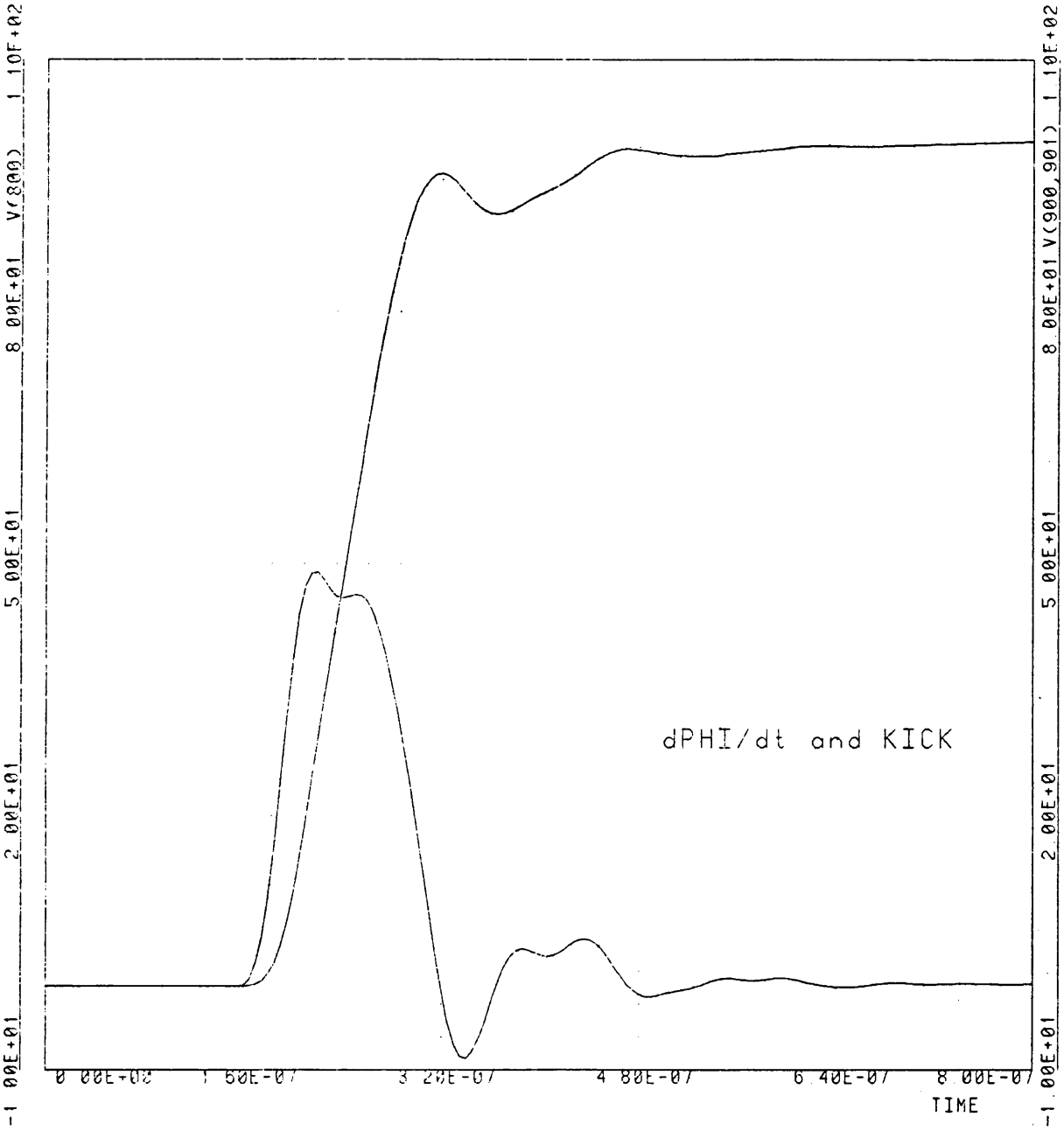

FIG. 14 SPICE Results.

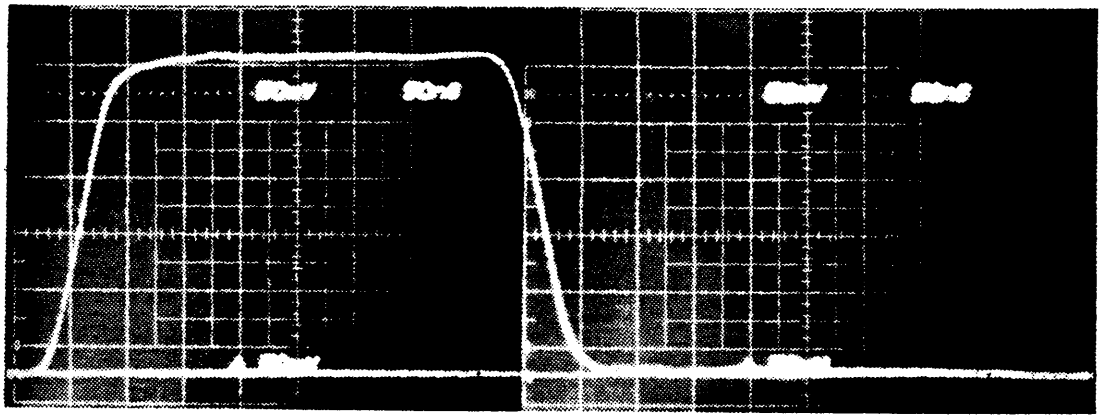

FIG. 15 H.V. $\int$Bdl.

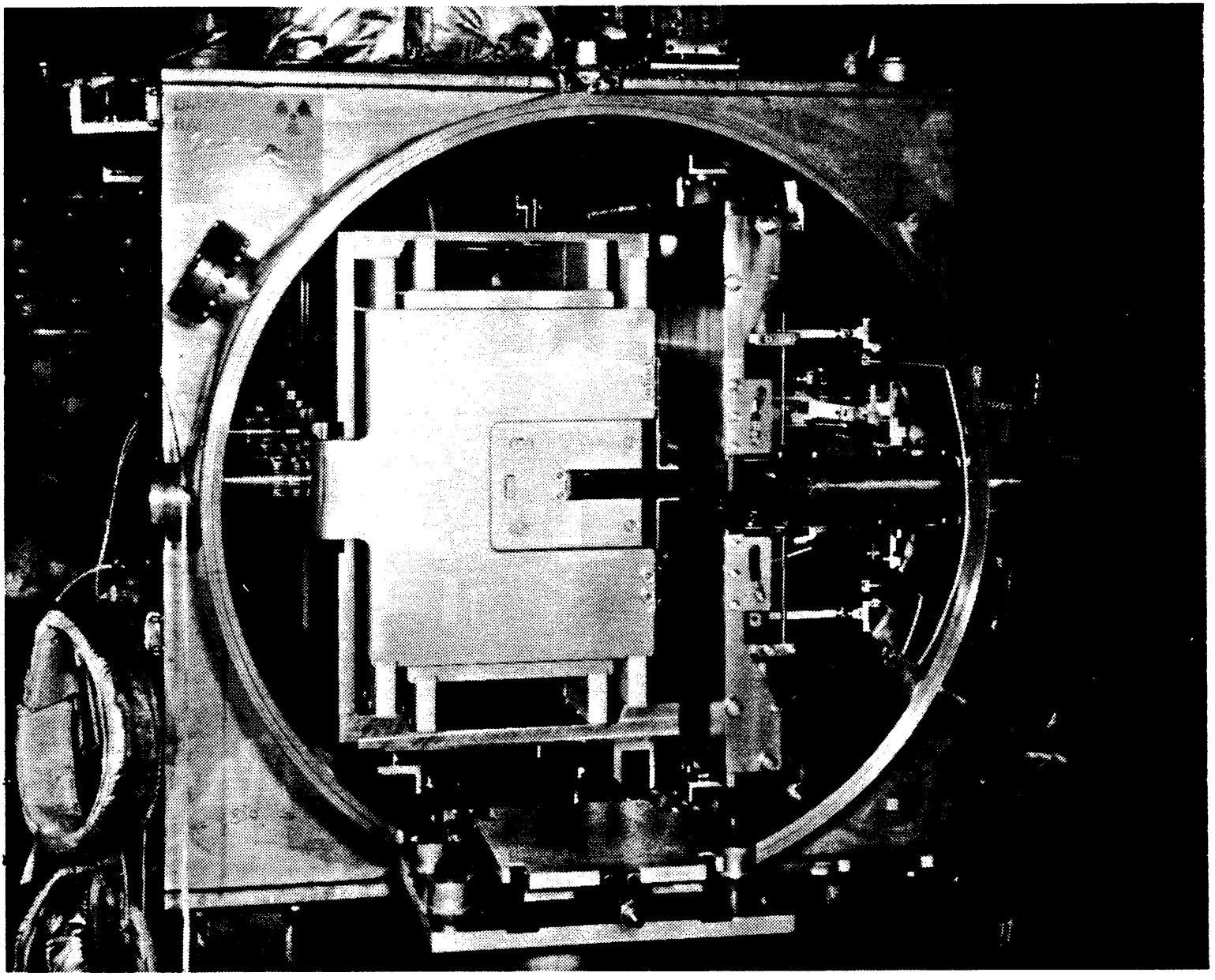

FIG. 16 Tank K4

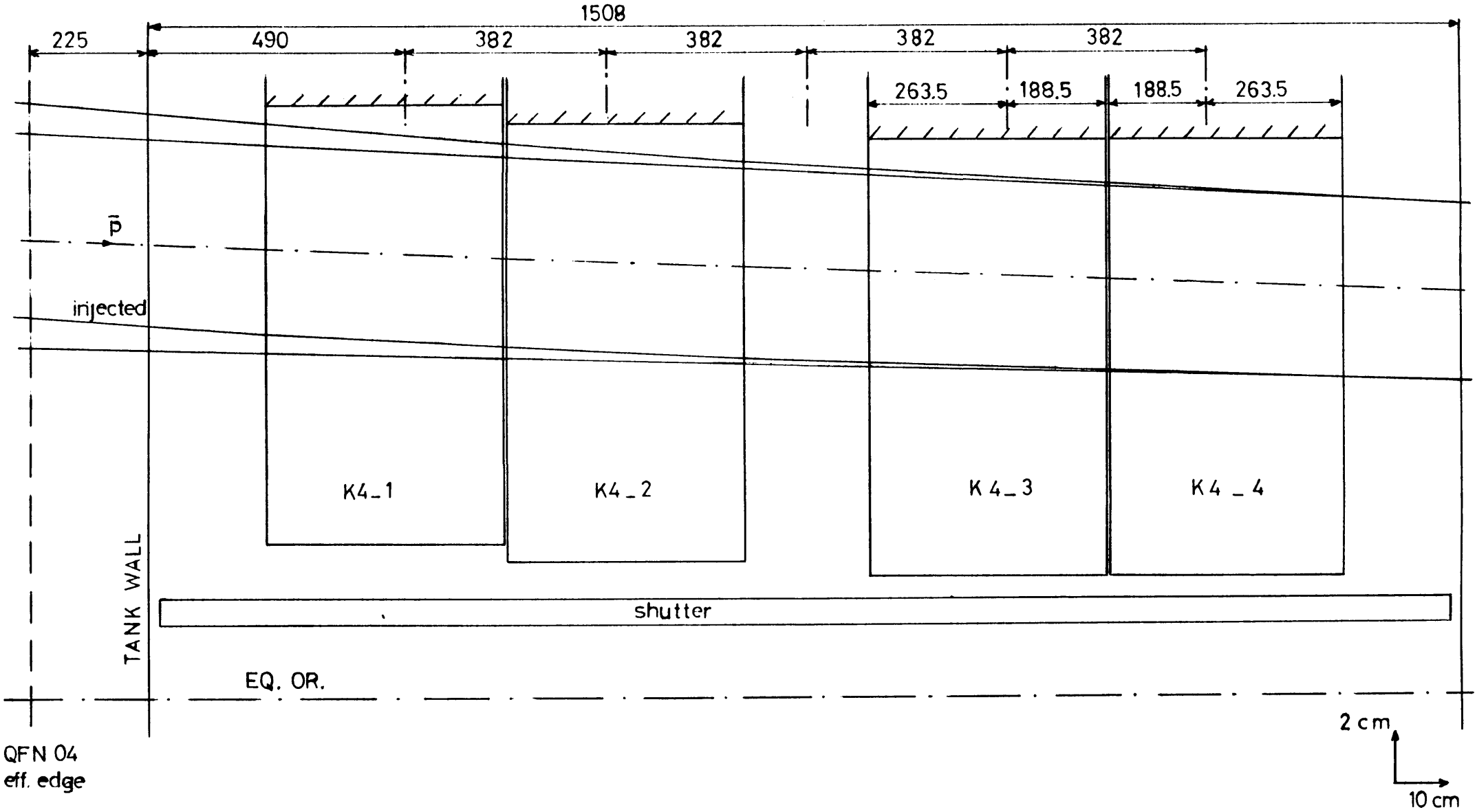

FIG. 17 Magnet disposition in K4.